



## FACULTY OF SCIENCE



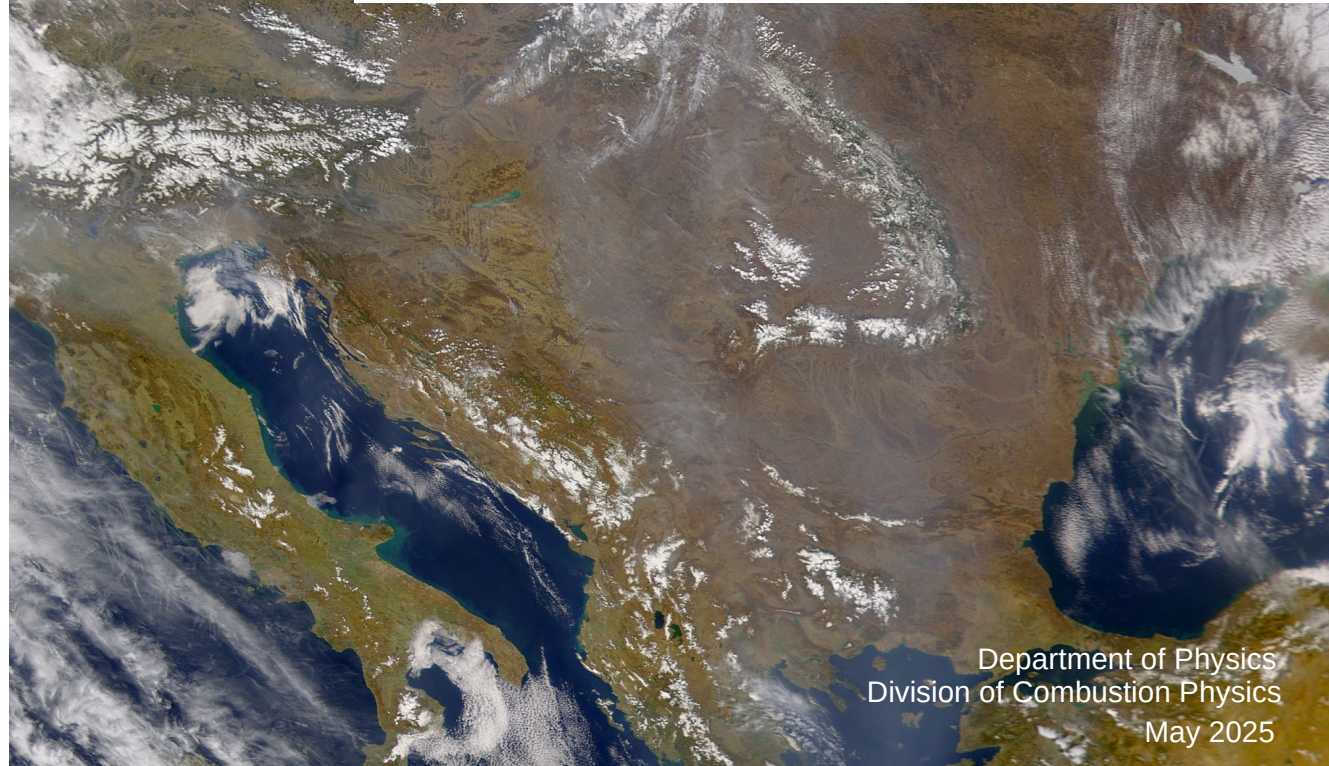
# Relation Between High Pressure Blocking and Aerosol Concentrations in Southern Sweden

Fredrik Bergqvist

---

Thesis submitted for the degree of Bachelor of Science  
Project duration: 2 months

Supervised by Moa Sporre



Department of Physics  
Division of Combustion Physics  
May 2025



## Abstract

High-pressure blocking events are anticyclones that persist over a region for a long time. The event prevents vertical mixing of air pollutants due to the subsidence inversion created by the adiabatic compression of air during the anticyclone. This study investigated the relationship of aerosol concentrations during periods of high-pressure blocking events in southern Sweden for the rural location of Vavihill and the urban location of Malmö. A total of 247 high-pressure blocking events were found in Vavihill and Malmö between 1995 and 2024. The requirements for a high-pressure blocking event were: A pressure above 1014 hPa, the event lasting for at least 5 days, and has a maximum amount of rainfall of  $0.5 \text{ mm h}^{-1}$ . These criteria had to be fulfilled for the initial five days in both locations with a maximum time difference of 5 h. The high-pressure blocking event was compared to mean  $\text{PM}_{2.5}$  concentrations from the same locations for each hour since the beginning of the event. The data was also sorted according to wind direction, season, and pressure strength for further analysis. Using Mann-Kendall statistics and standard deviations, the data showed a significant increase of  $\text{PM}_{2.5}$  for both locations during periods of high-pressure blocking. Higher  $\text{PM}_{2.5}$  concentrations were observed in Malmö due to larger local emissions. Peak aerosol levels were achieved after 8 to 13 days, indicating an accumulation of aerosols during the event in both locations. The investigation showed a stronger increase with winds from the southeast, indicating advective transport of aerosols to the region, although local emissions also played a significant role. This was supported by the findings of the seasonal and pressure strength dependencies, where a stronger high-pressure blocking events showed the highest levels of  $\text{PM}_{2.5}$ . Although no increase in the frequency of high-pressure blocking events was found in the region, the impact on air quality from high-pressure blocking events is still crucial. These results show how aerosol concentrations depend on atmospheric events in the region .

**Keywords:** Aerosols,  $\text{PM}_{2.5}$ , high-pressure blocking, Mann-Kendall, southern Sweden

## Acknowledgments

Thank you, Moa Sporre, for the guidance through this thesis.

## Abbreviations

**PM<sub>2.5</sub>** Small particulate matter with an aerodynamic diameter less than 2.5 µm.

**HFA** A recurring high-pressure blocking event, known as the Fennoscandian High.

**SEA** Another recurring high-pressure blocking event, known as the Southeast Anticyclone.

**HM** Another recurring high-pressure blocking event, known as the Central European High.

## Contents

<b>1</b>	<b>Introduction</b>	<b>1</b>
1.1	The Physics Behind High-Pressure Systems . . . . .	2
1.2	The Origin of Aerosols . . . . .	4
1.3	Aerosol Concentrations During High-Pressure Blocking Events . . . . .	4
<b>2</b>	<b>Method</b>	<b>6</b>
2.1	The Data Handling and Devices . . . . .	6
2.1.1	The Aerosol Data and Measurements . . . . .	6
2.1.2	The Meteorological Data and Measurements . . . . .	7
2.2	The Identification of High-Pressure Blocking Events . . . . .	8
2.3	The Data Analysis . . . . .	9
2.4	Statistical Evaluation and the Mann-Kendall Test . . . . .	10
<b>3</b>	<b>Results</b>	<b>11</b>
3.1	The Change in Aerosol Concentrations . . . . .	11
3.1.1	The Change in Aerosol Concentrations Depending on Wind Direction . . . . .	12
3.1.2	The Change in Aerosol Concentrations Depending on Season . . . . .	14
3.1.3	The Change in Aerosol Concentrations Depending on Pressure Strength . . . . .	15
3.2	The Frequency of High-Pressure Blocking Events . . . . .	16
<b>4</b>	<b>Discussion</b>	<b>18</b>
4.1	Why an Increase Occurs After 8-13 Days for Stronger High-Pressure Systems . . . . .	18
4.2	Particle Advection Versus Local Emissions . . . . .	18
4.3	Differences Between the Urban and Rural Locations . . . . .	19
<b>5</b>	<b>Conclusion</b>	<b>20</b>
<b>6</b>	<b>Outlook</b>	<b>21</b>

# 1 Introduction

It is common knowledge that Earth's increasing temperature has many side effects. One such effect is the increase in frequency of extreme weather phenomena [2]. One such phenomenon, which lacks extensive research, is high-pressure blocking events. A high-pressure blocking event is an anticyclone that covers an area for a prolonged period of time and often blocks other types of weather, hence the name. This results in limited cloud formations and a pronounced daily temperature variation [3]. However, an anticyclone is also associated with slower air movement, causing the air to remain stagnant. This can lead to an accumulation of air pollutants such as aerosols [4].

To investigate the relationship between aerosols and high-pressure blocking events, one must analyse periods of high-pressure blocking and examine the concentration of aerosols during these periods. Thus, the aim of this thesis is to: identify a suitable method for detecting periods of high-pressure blocking using pressure data from the *Swedish meteorological and hydrological institute* (SMHI); analyse these periods in relation to PM<sub>2.5</sub> levels from rural (Vavihill, Svalöv, Skåne County) and urban (Malmö, Skåne County) areas. Additional relevant data, such as wind direction, season, and pressure strength will be examined to gain a comprehensive understanding of high-pressure blocking events and their characteristics. This thesis will also explore the frequency of high-pressure blocking events to determine whether this weather phenomenon is becoming more common, which is particularly important if a positive correlation with aerosol levels is found.

## 1.1 The Physics Behind High-Pressure Systems

Anticyclones are meteorological high-pressure systems in which air sinks toward the ground, creating high pressure [5]. This occurs due to the convergence of air from all directions at high altitudes, which forces the air to move downward. The descending air undergoes adiabatic compression, resulting in an increase in the energy of the air molecules, or, in other words, a higher temperature. This rise in energy inhibits cloud formation, as warmer air can hold more moisture. The absence of clouds allows solar radiation to significantly impact the temperature during an anticyclone. Consequently, this leads to a large temperature difference between day and night, with summer anticyclones being associated with high temperatures and winter anticyclones with low temperatures.

Under normal conditions the temperature of the air in the atmosphere decreases with the altitude, due to the adiabatic expansion of the air. The cooling per altitude is called the environmental lapse rate and makes it possible for vertical wind movement to occur, when a slight imbalance is introduced to the system. During an anticyclone, adiabatic compression of the air occurs as the air descends. This increases the temperature at lower altitudes. However, this downward movement of air does not reach the ground due to the friction opposed by buildings, forests, valleys, and other obstacles that creates friction by disrupting the airflow. Thus, the downward draught will spread out a few hundred meters above the ground and not mix with the air that lies closest to the ground. Since the air closest to the ground remains cool, while the air a few hundred meters up is warmer from the adiabatic compression, an inversion of the environmental lapse rate will be created. This process is called a subsidence inversion and will prevent air mixing between the ground level and the upper layers of the atmosphere [6].

Another type of inversion occurs during the night as the air closer to the ground loses heat due to the outgoing radiation from the Earth. This process is especially strong due to the absence of clouds during the anticyclone. This creates a ground inversion layer, where the air temperature increases with height closer to the surface [7]. This ground inversion, created from the daily cycle, also prohibits vertical air movement in the atmosphere.

A high-pressure blocking period refers to a prolonged anticyclone characterized by higher surface pressure covering a large area [3]. Since the blocking event extends over a vast region, the pressure gradient remains small due to minimal fluctuations. As a result, the wind tends to be calm. A blocking period is typically defined as lasting between five and ten days, although some events can persist even longer [8]. However, no single definition of high-pressure blocking events exists [3]. While the concept has been recognized in meteorology for over a century, the long-term consequences of blocking events are not yet fully understood. High-pressure blocking periods are more common in the Northern Hemisphere compared to the Southern Hemisphere. Research has indicated that the frequency of blocking periods has increased in recent years [3].

Recurring anticyclones can be classified into Hess and Brezowsky macrocirculation types, such as the Fennoscandian High (HFA), the Southeast Anticyclone (SEA), and the Central European High (HM) [9]. HFA is centred on the Fennoscandinavian Peninsula (Norway, Sweden, Finland, and western parts of Russia) and is a recurring

anticyclone during the winter. This anticyclone is known for blocking air masses from the Atlantic, causing colder periods in the region. The SEA is a recurring anticyclone with its geographical center in southeastern Europe (the Balkans and western Türkiye). This anticyclone is most frequent during the summer months and is associated with heat waves. The HM is centred in central Europe (Germany, Poland, the Czech Republic) and occurs during both the summer and winter months.

To explain the air movement during an anticyclone the Navier-Stokes equation

$$\frac{\partial \vec{v}}{\partial t} + (\vec{v} \cdot \nabla) \vec{v} = \vec{g} - \frac{\nabla p}{\rho} - 2\vec{\Omega} \times \vec{v}, \quad (1)$$

can be used. The first term in Equation 1 corresponds to the local acceleration of the air, the second term corresponds to the convective acceleration of the air, the third term is simply the gravitational acceleration, the fourth term describes the force from the pressure gradient and the last term describes the Coriolis force. Since the aim is to examine the stable solution of this equation, we can assume that the local acceleration is zero. The weather system is a large scale system with the size of hundreds of kilometres, the speed is in the tens of meters per second and the Coriolis term is in the order of  $0.5 \times 10^{-4} \text{ s}^{-1}$ . Using this information one can observe that the size of the convection term is negligible in comparison to the Coriolis term. Lastly, one can assume the wind to be in the horizontal plane since vertical movement is a lot slower, providing a definition of the wind vector as  $\vec{v} = (v_x, v_y, 0)$ . The Coriolis term can be approximated by considering only the vertical component as  $\vec{\Omega} = (0, 0, \Omega_z)$ , since the horizontal components are negligible and Earth's rotation primarily projects along the vertical axis, causing deflections in the horizontal plane. The Navier-Stokes equation is thus simplified in the case of a stable large scale weather systems to

$$0 = -\frac{\nabla p}{\rho} - 2\vec{\Omega} \times \vec{v}, \quad (2)$$

where the gravity is neglected since it lies in the vertical plane while the wind lies in the horizontal plane. Solving for the horizontal velocity components from this equation one obtains the solution

$$v_x = -\frac{1}{2\rho\Omega_z} \frac{\partial p}{\partial y} \text{ and } v_y = \frac{1}{2\rho\Omega_z} \frac{\partial p}{\partial x}. \quad (3)$$

Examining the vorticity of the horizontal wind, one obtains

$$(\nabla \times \vec{v})_z = \frac{1}{2\Omega_z \rho} \nabla^2 p, \quad (4)$$

where the definition of the anticyclone (the pressure is strongest in the center) implies that  $\nabla^2 p$  is negative. Since  $\nabla^2 p$  is negative the vorticity is also negative, implying that the anticyclone rotates clockwise in the Northern Hemisphere. Since anticyclones exhibit winds rotating clockwise around their center, the winds from HFA, SEA, and HM tend to blow toward southern Sweden from the south, east and west. The transport of airborne pollutants, such as ozone, can occur via these winds [10]. Consequently, it can be hypothesized that other airborne aerosols, such as PM<sub>2.5</sub>, should also be transported through these wind patterns.

## 1.2 The Origin of Aerosols

The concentration of aerosols in the air can be measured by the combined mass of the particulate matter per volume. However, it is important to specify which types of particles are being measured, where PM<sub>2.5</sub> (particulate matter with an aerodynamic diameter of 2.5 µm or less) is a common choice due to its significant health impacts and its ability to be transported by the wind. Although aerosols can form naturally in the atmosphere, the primary sources in urban and suburban Europe include solid fuel combustion for domestic heating, industrial activities, and road transportation [11]. Particulate contributors to PM<sub>2.5</sub> include sulphur dioxide (SO<sub>2</sub>) and soot (black carbon), both originating from the burning of fossil fuels. The European Union set an annual mean limit for PM<sub>2.5</sub> concentrations at 25 µg m<sup>-3</sup> in 2008, although the WHO suggested a much lower threshold of only 5 µg m<sup>-3</sup> [11]. In 2022, the EU mean limit threshold was exceeded in several countries, including Croatia, Bosnia and Herzegovina, Italy, Poland, North Macedonia, and Türkiye [11].

Studies have demonstrated a correlation between elevated PM<sub>2.5</sub> concentrations and an increased risk of respiratory, cardiovascular, and cerebrovascular diseases, as well as diabetes [12]. A Danish study on 49 564 individuals between 1993 and 2015 showed that for every 5 µg m<sup>-3</sup> increase in aerosol concentrations the hazard ratio increased by 1.29 [13]. Thus, for every 5 µg m<sup>-3</sup> increase in PM<sub>2.5</sub> the risk of dying from cardiovascular diseases increased by 29 %. Further studies on PM<sub>10</sub>, which is a closely related to PM<sub>2.5</sub>, showed that in the age group of 75-84 mortality increased 36 % and 106 % in the age group 85+ during heat waves associated with high PM<sub>10</sub> concentrations [14].

## 1.3 Aerosol Concentrations During High-Pressure Blocking Events

During an high-pressure blocking event the environmental lapse inversion, especially the subsidence inversion, close to the ground prohibits vertical air mixing during the atmospheric layers closest to the ground. If aerosols are produced at ground level during this high-pressure blocking event, this would imply that the aerosols would not disperse vertically, implying a higher concentration on the ground level. Thus, one would expect higher concentrations of PM<sub>2.5</sub> during high-pressure blocking events. Chinese studies have shown that the vertical dispersion of aerosols during high-pressure blocking events are inhibited, increasing the concentration of PM<sub>2.5</sub> in cities [4].

Since aerosol emissions are particularly high in central European countries such as Poland, anticyclonic winds from the south and east from HFA, SEA, and HM are expected to increase PM<sub>2.5</sub> concentrations in southern Sweden [11]. These aerosols would be transported to southern Sweden via southerly to easterly winds during the anticyclone, which can be seen in Figure 1. If this occurs during a high-pressure blocking event, the aerosols may accumulate over the region while continuously being advected by southerly and easterly winds.

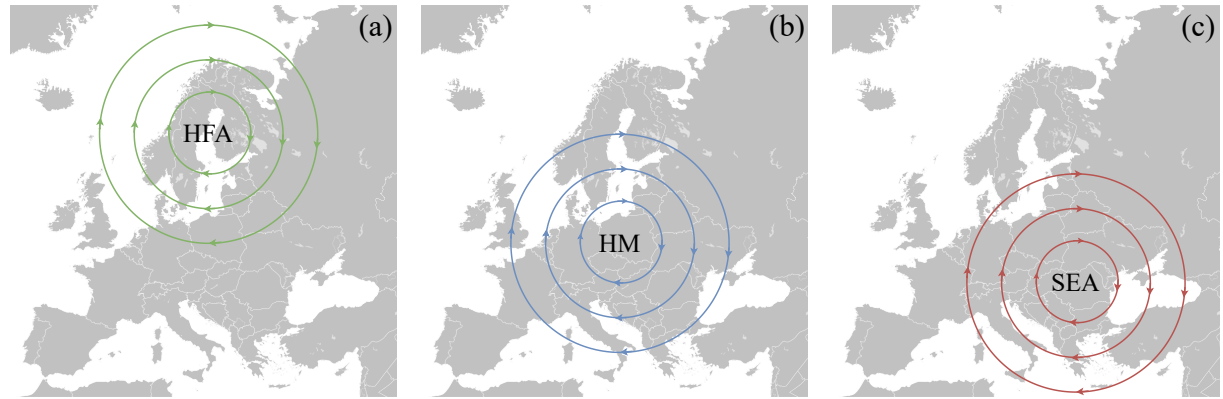


Figure 1: These streamline maps show the air movement during the HFA, HM, and SEA blocking events [15]. The figures only show the general streamlines of the Brezowsky macrocirculation types, meaning that the real world anticyclones would not be perfectly circular.

## 2 Method

### 2.1 The Data Handling and Devices

The meteorological data was downloaded from the SMHI's website as CSV files. The data included hourly atmospheric pressure data, hourly rain data, and hourly wind data (speed and direction). Hourly aerosol data as PM<sub>2.5</sub>, measured over one-hour intervals, was also downloaded. Since the purpose of this project was to analyse aerosol concentrations in southern Sweden during high-pressure blocking events, one urban and one rural site were selected. The locations were chosen based on their classification as rural or urban and the length of time the stations had been in operation, where more data was considered better.

#### 2.1.1 The Aerosol Data and Measurements

The rural measuring station in the county of Skåne with the most data was Vavihill located in Svalöv, southern Sweden. This station was active from September 28, 1999, to November 15, 2017. However, due to missing data on some days, only 57 % of the period contained non-missing values. Additionally, between 2017 and 2018, the Vavihill station was relocated to nearby Hallahus, where it operated from May 10, 2018, to December 31, 2022, with 93 % of the period containing non-missing values. Combining these datasets resulted in a total of 5371 days of hourly data. For an urban location in the county of Skåne, Malmö Rådhuset had the most data, with measurements recorded from June 3, 1999, to December 31, 2023. Here, 90 % of the recorded values were non-missing, resulting in 8074 days of data.

The measurement device used at Vavihill was the ambient particulate monitor TEOM 1400. This monitor continuously collects airborne particles less than 2.5 µm onto a filter and measures their mass using an oscillating microbalance technique [16]. The oscillating microbalance works by vibrating at a natural frequency, which changes as particles accumulate on the filter. Since this frequency shift is proportional to the mass of the particles, their total mass can be calculated. The precision of the monitor was  $\pm 1.5 \mu\text{g m}^{-3}$ . Thus, the monitor provides high precision and stable measurements. However, a key limitation is that it cannot distinguish between different types of particles, as it only measures total mass.

When the measuring station was moved to Hallahus, the measuring device was updated to the fine dust analysis system Palas FIDAS 200. This device works by an optical aerosol spectrometer which samples particles from an isokinetic inlet through a polychromatic light-scattering channel where the scattering angles and intensities were measured. [17]. This results in a high accuracy of  $\pm 0.1 \mu\text{g m}^{-3}$ , indicating an improvement from the previous device.

The monitoring station in Malmö used several measuring devices over time, in conjunction with other equipment. Between the start of the monitoring and January 1, 2009, the TEOM 1400 monitor was used. From January 1, 2009, to December 31, 2015, the TEOM 1400, FDMS, and 8500 B or CB dryer were employed. Between January 1, 2016, and December 31, 2021, the TEOM 1405F and FDMS systems, along with the 8500 B, were in use. Finally, from January 1, 2022, the Palas FIDAS 200 monitor replaced the earlier systems. The FDMS (Filter Dynamics Measurement System) is a dynamic filter measurement system that enhances measurements by accounting for volatile and semi-volatile particles [18]. The CB dryer and 8500 B were air dryers used to prevent moisture from entering the measurement devices, ensuring accurate data by avoiding potential interference caused by water vapour.

### 2.1.2 The Meteorological Data and Measurements

The choice of atmospheric pressure measurement station was Helsingborg, located 25 km from Vavihill and 49 km from Malmö. This location was chosen based on its proximity to both PM<sub>2.5</sub> measuring stations, the fact that neither Malmö nor Vavihill have pressure measurements from this period, and the fact that the station has been in use from August 2, 1995, with measurements taken every hour without any missing values. The period used for this station was from start until October 10, 2024. This station thus covers the entire period of the PM<sub>2.5</sub> data. Although the data was measured at a certain altitude, the data was displayed as recalculated sea-level pressure.

The barometer that has been in use for Helsingborg is a Vaisala PTB201A for the entire period, except for the periods from April 15, 2015, to April 17, 2025, and from September 19, 2004, to May 23, 2014, when a Vaisala PTB220 was used instead. Even then, the device has been serviced every year or every other year. The PTB201A digital barometer operates using a silicon capacitive absolute pressure sensor, providing stable and accurate pressure values [19]. The sensor functions by means of a flexed diaphragm inside a capacitor that bends in response to air pressure, causing a change in the capacitor's distance and thus a variation in the current. This device measures pressure in the range of 600 hPa to 1100 hPa, with an accuracy of  $\pm 0.3 \text{ hPa}$ . Errors in the device may arise due to environmental factors, such as exposure to condensing gases. The Vaisala PTB220 digital barometer operates in a similar manner but offers a wider measurement range of 500 hPa to 1100 hPa, with an improved accuracy of  $\pm 0.15 \text{ hPa}$  [20].

The relevant rain and wind data were gathered from two different stations. For Vavihill, the station at Hörby, located 35 km away, was used, and for Malmö, a weather station just 6 km away was used. The weather station at Hörby was chosen instead of Helsingborg since neither Vavihill nor Hörby are located along the coast, whereas Helsingborg is. Coastal regions experience a daily cycle of sea breezes and land breezes, which alter the wind direction. The wind and rain data from Hörby were measured from August 1, 1995, to October 1, 2020, with measurements taken every hour without any missing values. The Hörby station was temporarily relocated for a short period in 2021. The rain data from Malmö was measured from November 21, 1995, and the wind data from

January 1, 1990, with both measurements ending on December 31, 2020. These stations did not lack any data.

The wind data from both Hörby and Helsingborg used the high-performance wind sensor Vaisala WAA15A for the wind speed and Vaisala WAV15A for the wind direction. These instruments were serviced and calibrated every year or every other year, and had been in use since 1995. The WAA15A anemometer measured wind speed with an accuracy of  $\pm 0.17 \text{ ms}^{-1}$ , and the WAV15A wind vane measured the wind direction with an accuracy better than  $\pm 3^\circ$  [21]. The WAA15A anemometer works by a rotating chopper disc that interrupts an infrared beam, resulting in a laser pulse proportional to the wind speed. The WAV15A wind vane uses a counterbalanced vane with an optical disc. When the vane turns, infrared LEDs detect the change in angle with the disc and phototransistors, resulting in a precise measurement of the wind angle. For rain monitoring, the Geonor T200 device had been in use for all stations since 1995. Like the wind monitor, this device had been serviced and calibrated every year or every other year. This device works by measuring precipitation with a vibrating wire sensor that detects weight changes from the water droplets [22]. The device has a measurement accuracy better than  $\pm 0.1 \text{ mm}$ .

The final task of this study was to evaluate if high-pressure blocking events had become increasingly more common. For this evaluation, atmospheric pressure data from Ängelholm airport was used instead of Helsingborg due to the pressure data from Ängelholm being active from January 5, 1946, meaning it has been in service for 49 years longer than that from Helsingborg. The data period used was from start until October 1, 2024. This station is located 44 km from Vavihill and 76 km from Malmö. However, the pressure values differed only by a mean of 0.25 hPa and a standard deviation of 0.20 hPa between December 1, 1995 to October 1. The rain data was also expanded by using daily rain data from Ängelholm since this data was gathered from January 18, 1947, to November 30, 2001. To obtain the maximum amount of the rain data the data from Ängelholm was used together with the nearby station of Tånga. This station is located 12 km away and had been in use since December 19, 1973. For this station the period used was from start until August 31, 2024 with daily rain data. The rain measurements in Tånga was measured manually by a beaker located on a field. Thus, errors in this measurement were higher than the digital measurement devices.

## 2.2 The Identification of High-Pressure Blocking Events

To evaluate the occurrence of high-pressure blocking event for Vavihill or Malmö, the rain data and atmospheric air pressure were used. For a period to be defined as a high-pressure event, the atmospheric pressure had to be over 1014 hPa, and the rainfall had to be less than  $0.5 \text{ mm h}^{-1}$ . These values were based on the fact that 1014 hPa was the mean atmospheric pressure from Helsingborg, and  $0.5 \text{ mm h}^{-1}$  was chosen since this is considered light rain. The rain-limit was set to  $2 \text{ mm d}^{-1}$  in the case where daily precipitation was used instead. This value was chosen since it corresponds to a small amount of rainfall for a day. The reason for not using a rain limit of  $12 \text{ mm d}^{-1}$  is that it corresponds to a large amount of precipitation, whereas  $2 \text{ mm d}^{-1}$  does not. The choice of  $0.5 \text{ mm h}^{-1}$  for hourly data is motivated by the fact that continuous light rain over a 24-hour period is very rare. As a result,

daily precipitation levels seldom reach  $12 \text{ mm d}^{-1}$ , and are more commonly around  $2 \text{ mm d}^{-1}$ . Since a high-pressure blocking event covers a large geographical area, and Vävihill and Malmö are located close to each other, a blocking event observed at one site should also be detectable at the other. To account for this, all identified high-pressure blocking events at one location were required to correspond to an event at the other location within a maximum time difference of 5 h for the initial five days. For a high-pressure event to be considered a high-pressure blocking event, the criteria for a high-pressure event had to persist for at least 120 h (5 days). This value was chosen since a 5-day limit is often considered when classifying high-pressure blocking events [3].

### 2.3 The Data Analysis

The evolution of  $\text{PM}_{2.5}$  during the high-pressure blocking events were evaluated by calculating the mean and standard deviation of  $\text{PM}_{2.5}$  for each hour of the high-pressure blocking events, to evaluate the average progression of aerosols over time. This was done using the Python packages NumPy and pandas. Since the high-pressure blocking events varied in length a minimum of eight events was allowed when taking the mean and standard deviation on the  $\text{PM}_{2.5}$  data. The mean PM value was then compared with the mean  $\text{PM}_{2.5}$  value during periods without high-pressure blocking events, as well as with the EU annual mean limit for  $\text{PM}_{2.5}$ . Due to the lack of  $\text{PM}_{2.5}$  data during some periods, a filter was applied, stating that a period needed 85 %  $\text{PM}_{2.5}$  coverage in order to be analysed.

The data was sorted in different ways to explore how the  $\text{PM}_{2.5}$  concentration depended on different parameters. Firstly, the data was sorted into one of four wind categories: northeast ( $310^\circ$  to  $70^\circ$ ), southeast ( $70^\circ$  to  $190^\circ$ ), west ( $190^\circ$  to  $310^\circ$ ), and no specific direction. This was done by categorizing the data if 60 % of the wind directional data fell into one of these categories, with no wind being handled as a missing value.

Secondly, the data was sorted based on the season of the blocking. This was evaluated by taking the midpoint date of the blocking and categorizing the season by the month it occupied. December, January, and February were considered winter; March, April, and May were considered spring; June, July, and August were considered summer and September, October, and November were considered autumn. Lastly, the data was categorized based on the strength of the high-pressure blocking, where a weak high-pressure blocking event had a mean atmospheric pressure between 1014 hPa and 1020 hPa, an event had a mean atmospheric pressure between 1020 hPa and 1025 hPa, and an event had a mean atmospheric pressure over 1025 hPa.

The last task of this study was to evaluate whether high-pressure blocking events had become increasingly more common. This was evaluated in two different ways: by calculating the number of days under high-pressure blocking events per year, and the number and lengths of high-pressure blocking events per year. The number of days of blocking was also sorted by the season of the blocking to provide more insight into the nature of the high-pressure blocking events.

## 2.4 Statistical Evaluation and the Mann-Kendall Test

To evaluate statistical significance of the trends found in the study, the statistical Mann-Kendall test was used. The Mann-Kendall test was applied to evaluate whether the PM<sub>2.5</sub> mean during high-pressure blocking events had increased, and if so, by how much. The Mann-Kendall test is a non-parametric statistical test used to calculate the monotonic trend, the significance of the result and the linear trend of a dataset. This test is commonly used in climate physics due to the challenges posed by many parameters and complex distributions. The test works by calculating the difference between each time step in the dataset. The output will be a p-value below 0.05 if the test provides a significant result, meaning that the trend is unlikely to be caused by randomness. Kendall's  $\tau$ -value is used to evaluate the monotonic increase of the dataset, where -1 indicates a total monotonic decrease, 1 indicates a total monotonic increase, and 0 indicates no monotonic trend. The  $\tau$ -value can be summarized by the formula

$$\tau = \frac{C - D}{C + D}, \quad (5)$$

where  $C$  is the number of concordant pairs and  $D$  is the number of discordant pairs. If the result yielded a  $\tau$ -value above 0.5, the result was labelled as a clear increase. Sen's slope is a method of performing linear regression on the data. The method differs from the least squares method because it uses the median to calculate the slope. This ensures that outliers, which are common in weather data, do not affect the results. Sen's slope is calculated as

$$S_i = \frac{C_{i+1} - C_i}{t_{i+1} - t_i} \quad \text{Sen's slope} = \text{median}(S_i), \quad (6)$$

where  $i$  represents the indices,  $C$  represents the concentration of PM<sub>2.5</sub>, and  $t$  represents time. The program used for the Mann-Kendall test was the `pymannkendall` package in Python [23].

## 3 Results

### 3.1 The Change in Aerosol Concentrations

After applying the high-pressure blocking detection method to the data from Vavihill and Malmö for the entire period, a total of 213 high-pressure blocking events were identified between November 27, 1995 and September 22, 2024. For Vavihill 114 high-pressure blocking events of the original 213 were removed due to insufficient PM<sub>2.5</sub> data, as a filter requiring 85% data coverage was applied. This left 99 relevant high-pressure blocking events. For Malmö 48 high-pressure blocking events were removed due to insufficient PM<sub>2.5</sub> data, again applying the 85% data coverage filter. This resulted in 165 relevant high-pressure blocking events. An example plot showing periods of high-pressure blocking events can be seen in Figure 2. This figure provides insight into other categorization of high-pressure blocking events for the two different locations.

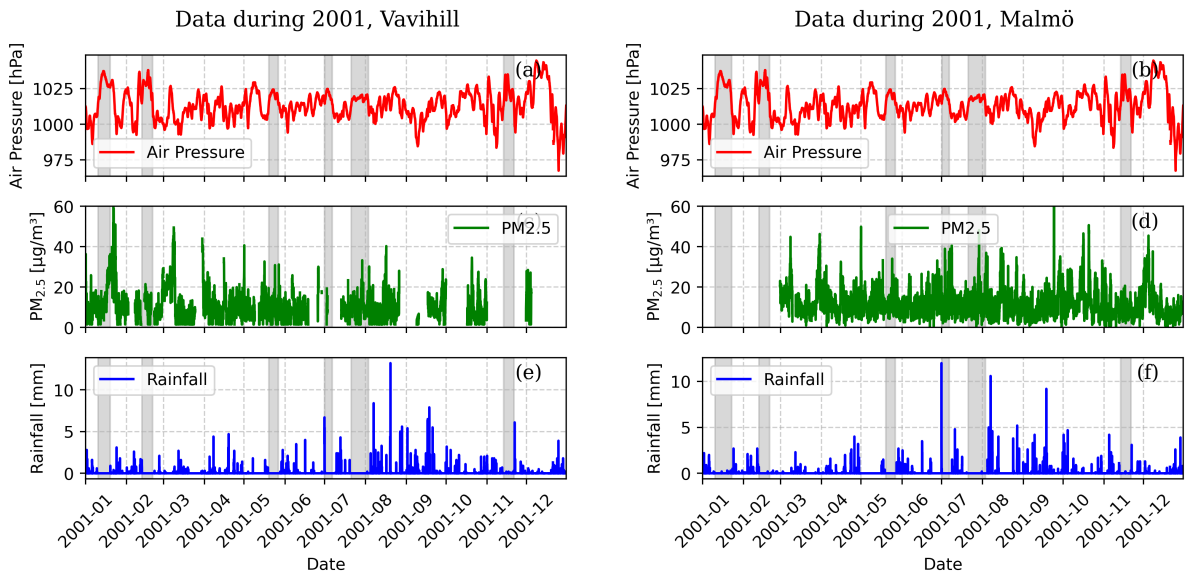


Figure 2: Example plots displaying the air pressure, PM<sub>2.5</sub> concentrations, and rainfall during the year 2001. The periods which were indicated as periods of high-pressure blocking events are shown in gray. This displays a normal yearly distribution of high-pressure blocking events using the described method.

The average change in PM<sub>2.5</sub> concentrations during periods of high-pressure blocking can be seen in Figure 3. The data is compared with the PM<sub>2.5</sub> mean taken from periods without high-pressure blocking events. An increase in PM<sub>2.5</sub> concentrations can be seen in Malmö from  $10 \mu\text{g m}^{-3}$  to a maximum of  $21 \mu\text{g m}^{-3}$  at day thirteen, and an increase from  $7 \mu\text{g m}^{-3}$  to a maximum of  $18 \mu\text{g m}^{-3}$  at day twelve can be seen in Vavihill. A stronger increase in Malmö is supported by the large  $\tau$ -value of  $\tau = 0.78$ , and slight lower  $\tau = 0.70$  in Vavihill. The Sen's slope values also indicate a stronger increase in Malmö  $3.0 \times 10^{-2} \mu\text{g m}^{-3} \text{ d}^{-1}$  compared to  $2.1 \times 10^{-2} \mu\text{g m}^{-3} \text{ d}^{-1}$  in Vavihill.

After the first five days, the number of high-pressure blocking events decreases, which is reflected in the increase in standard deviation. Figure 3–6 all provided significant result since all had a p-value approximately equal to 0.

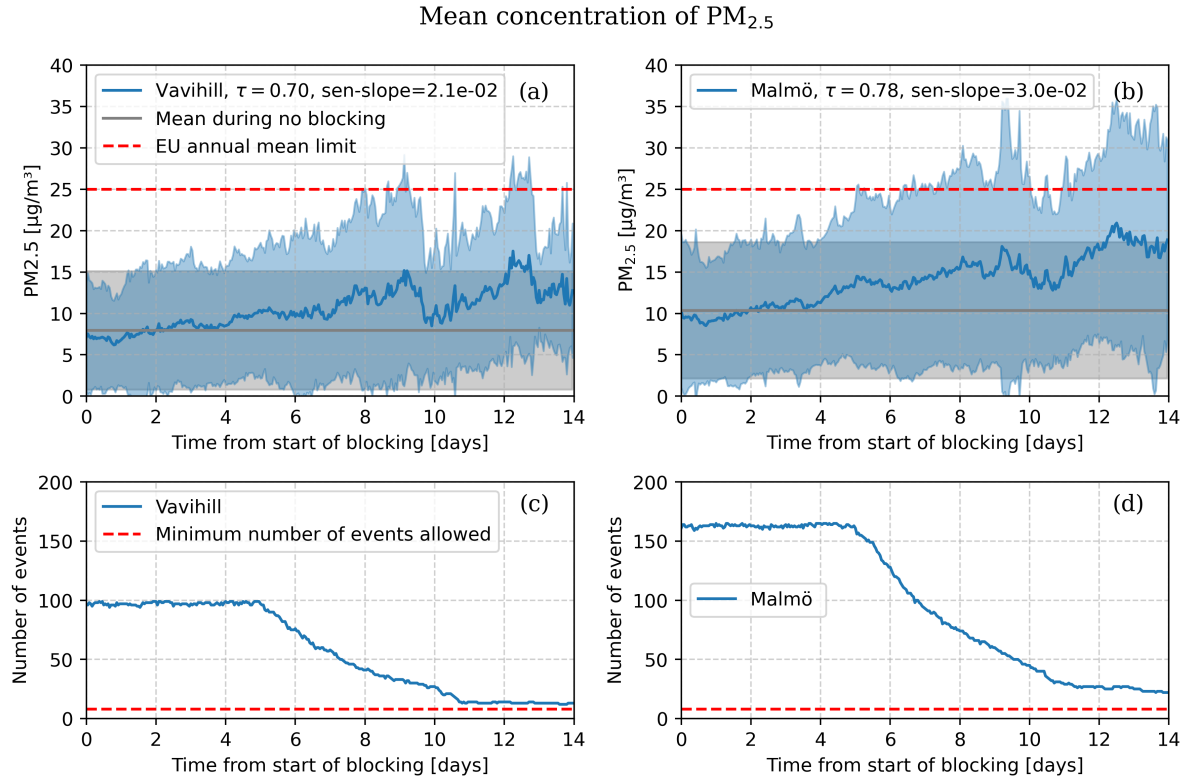


Figure 3: Comparison of mean PM<sub>2.5</sub> concentrations in Vävihill (a) and Malmö (b), highlighting differences between rural and urban air quality. The shaded region indicates the standard deviation of the data. The number of high-pressure blocking events used in the analysis can be seen in (c) and (d).

### 3.1.1 The Change in Aerosol Concentrations Depending on Wind Direction

The change in PM<sub>2.5</sub> concentrations in Vävihill and Malmö for different wind directions can be seen in Figure 4. In the case of Vävihill, 7.1% of the winds came from the northeast (310° to 70°), 27.3% from the southeast (70° to 190°), 23.2% from the west (190° to 310°) and 42.4% from no specific direction. In the case of Malmö, 7.9% of the winds came from the northeast (310° to 70°), 24.8% from the southeast (70° to 190°), 18.2% from the west (190° to 310°) and 49.1% from no specific direction.

One can observe similarities between the aerosol concentrations depending on wind directions for Vävihill and Malmö, although a larger increase can be observed in Malmö. When the wind filter was applied for the northeast direction, no strong increase or high levels of PM<sub>2.5</sub> were detected, as supported by the  $\tau$ -values being under 0.5 for Malmö, and no statical amount of data being found at Vävihill (a-b). In Vävihill for southeastern direction yielded  $\tau = 0.41$ , however there is a clear increase until day nine, where the levels suddenly drop (c). The  $\tau$ -value for the first nine days is  $\tau = 0.68$ , showing a clear increase. The southeastern direction for Malmö yielded a high

$\tau$ -value of  $\tau = 0.64$  and mean concentration exceeding the EU annual mean limit with a maximum concentration of  $26 \mu\text{g m}^{-3}$ (d). For the western wind direction, an increase in  $\text{PM}_{2.5}$  can be seen in Vävihill as supported by  $\tau = 0.57$  (e). The western wind direction for Malmö showed an increase until day eight, where it suddenly drops. Although elevated levels can be seen on day eight, one must note that the spread of the values is large (f).

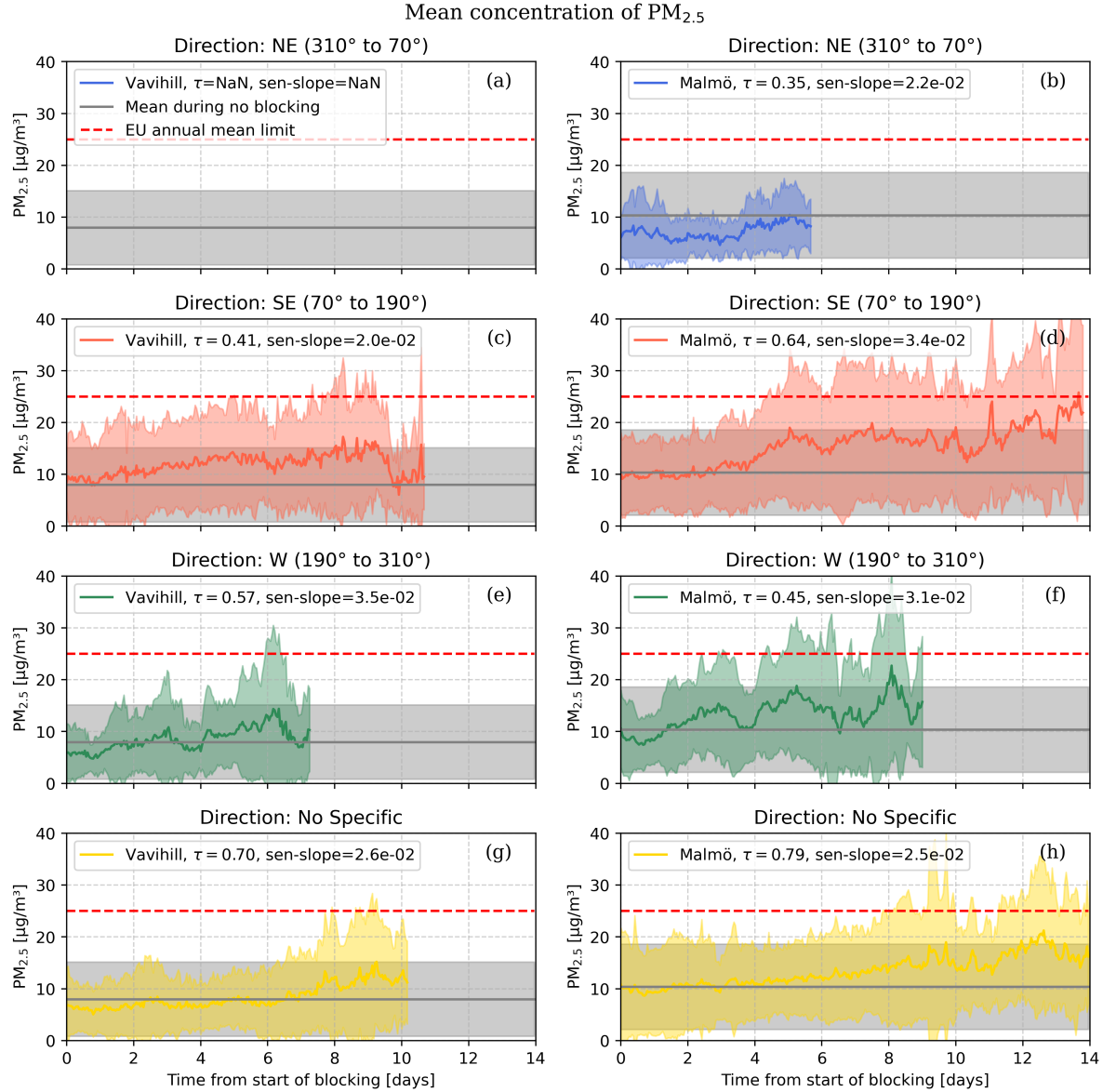


Figure 4: Plots showing how  $\text{PM}_{2.5}$  concentrations in Vävihill and Malmö evolve for different wind directions. A minimum number of blocking events was still put to eight, resulting in some directions having very little data.

### 3.1.2 The Change in Aerosol Concentrations Depending on Season

The seasonal change in concentrations of PM<sub>2.5</sub> can be seen in Figure 5. 19.8% of the events occurred during the winter, 32.8% during the spring, 19.8% during the summer and 27.6% during the autumn. From Figure 5 e-f, it is clear that the concentration during the summer for both Vavihill and Malmö does not show an increase nor high levels of PM<sub>2.5</sub>. A slight increase can be seen for the spring in both locations , with Vavihill going from 9 µg m<sup>-3</sup> to a maximum of 12 µg m<sup>-3</sup> and Malmö from 11 µg m<sup>-3</sup> to a maximum of 16 µg m<sup>-3</sup> (c-d). A larger increase can be seen during the autumn (g-h), where high levels of PM<sub>2.5</sub> can be observed towards the end of the period, with Vavihill going from 10 µg m<sup>-3</sup> to a maximum of 16 µg m<sup>-3</sup> and Malmö from 11 µg m<sup>-3</sup> to a maximum of 26 µg m<sup>-3</sup>. The winter in Vavihill and Malmö showed an increase in the PM<sub>2.5</sub> concentrations, with Malmö showing a much stronger increase which is supported by the large the  $\tau$ -value and the large Sen's slope during the (a-b).

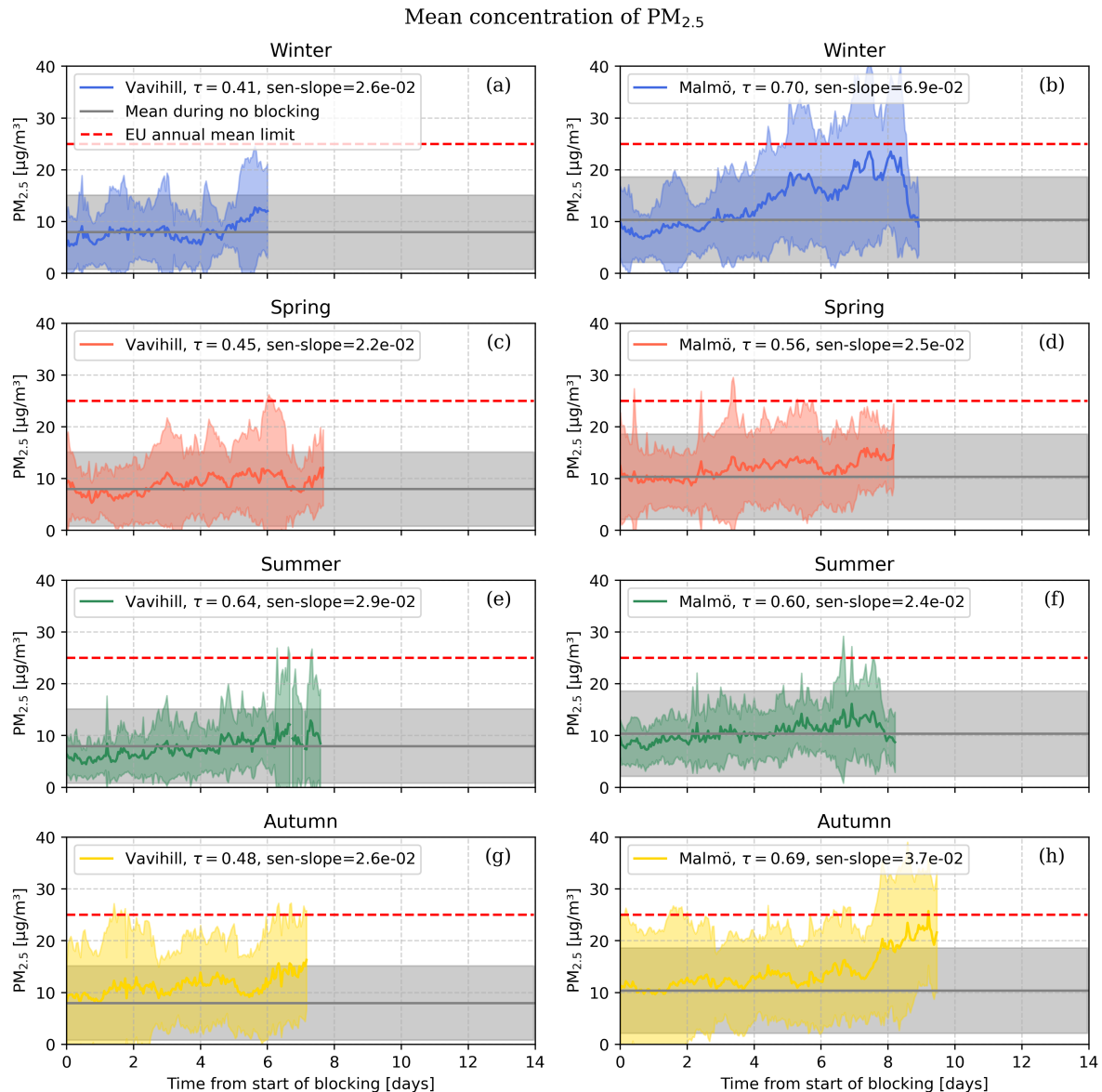


Figure 5: Plots showing PM<sub>2.5</sub> concentrations in Vavihill and Malmö for different seasons.

### 3.1.3 The Change in Aerosol Concentrations Depending on Pressure Strength

The increase in PM<sub>2.5</sub> concentrations depending on the strength of the high-pressure blocking event can be seen in Figure 6. In the case of Vävihill, 22.2% of the blocking events occurred with a mean pressure below 1020 hPa 45.5% occurred between 1020 and 1025 hPa and 31.3% occurred with a mean pressure over 1025hPa. In the case of Malmö, 17.0% of the blocking events occurred with a mean pressure below 1020 hPa 48.5% occurred between 1020 and 1025 hPa and 34.5% occurred with a mean pressure over 1025hPa.

From the plots, one can observe similar behaviour for the two locations. For the weaker high-pressure blocking events no clear increase can be seen for Malmö, nor highly elevated levels of PM<sub>2.5</sub> for neither location (a-b). In the case of medium strong high-pressure blocking events a stronger increase in Vävihill  $\tau = 0.62$  and weaker in Malmö  $\tau = 0.30$  can be seen. When observing both plots one can see an maxima around day nine, although the maxima in Malmö has a larger value spread (c-d). For the stronger high-pressure blocking events one can see a strong increase in the case of Malmö and in Vävihill, although the increase in Vävihill is slightly weaker. When viewing the plots (e) and (f) one observes that the levels of PM<sub>2.5</sub> in the case of Vävihill and Malmö exceed the normal range at day thirteen, where the mean reached the EU annual mean limit for Malmö. In Vävihill the values went from 9  $\mu\text{g m}^{-3}$  to a maximum of 21  $\mu\text{g m}^{-3}$  and in Malmö they went from 12  $\mu\text{g m}^{-3}$  to a maximum of 28  $\mu\text{g m}^{-3}$ .

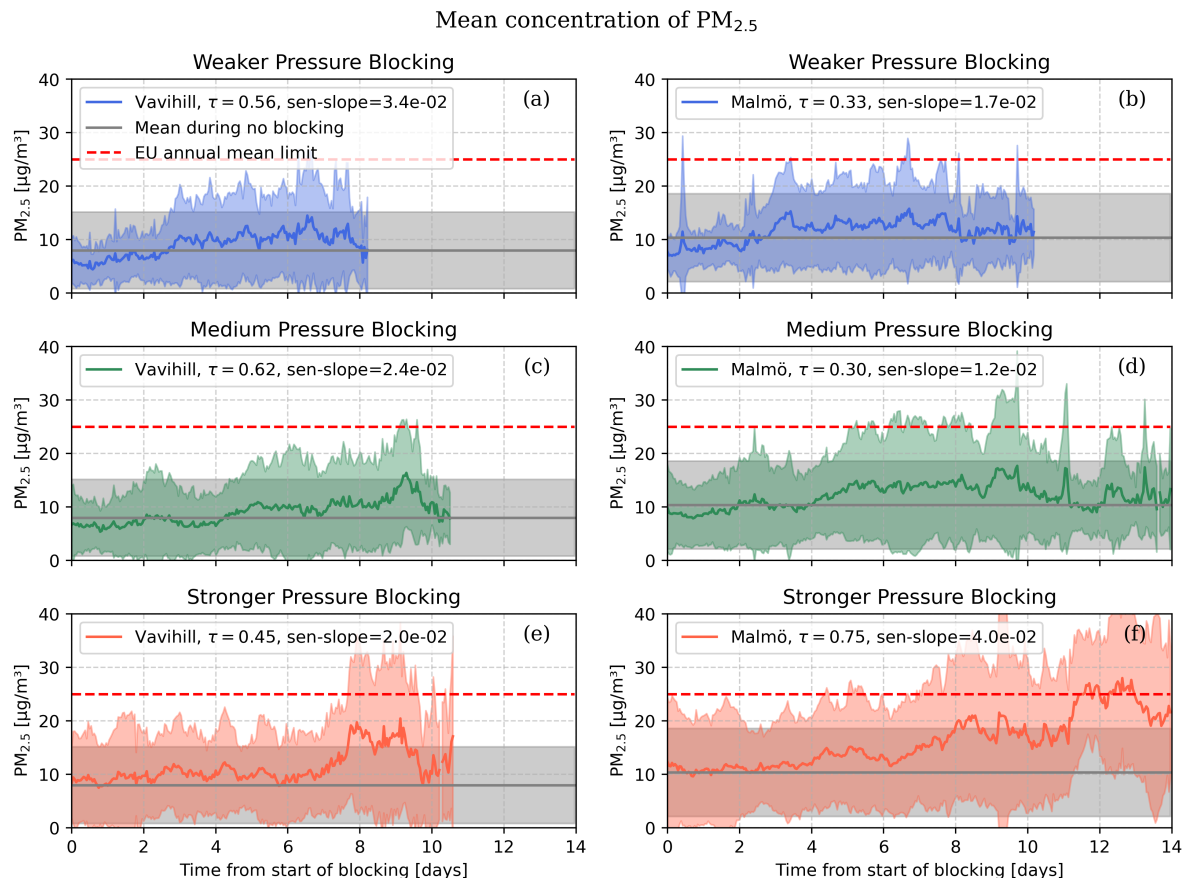


Figure 6: Plots showing PM<sub>2.5</sub> concentrations in Vävihill and Malmö for different pressure strengths for high-pressure blocking events.

From Figure 3–6 it is clear that the high elevations of PM<sub>2.5</sub> occur after eight to thirteen days. These results indicates that prolonged periods of high-pressure blocking events indicate an accumulative increase of PM<sub>2.5</sub>, which can be seen in Figure 3 where one can see that the combination of all the other plots resulted in a steady increase in the case of Malmö, and an increase in the case of Vavihill. The only case no increase is seen is when the wind direction is from the northeast (see Figure 4 a-b), which is not very common. This result indicates that for high-pressure blocking events one observes an increase in the concentration of PM<sub>2.5</sub> after eight to thirteen days regardless of the type of high-pressure blocking event, even though different types of high-pressure blocking events may differ in their specific increase. Especially strong increases with elevated PM<sub>2.5</sub> levels could be seen with winds from the southeast and even higher for stronger high-pressure blocking events.

### 3.2 The Frequency of High-Pressure Blocking Events

The last task was to determine whether high-pressure blocking events have become more common. When observing the number of high-pressure blocking events per year, no significant change in frequency could be seen (see Figure 7). Since the highest levels of PM<sub>2.5</sub> occurred toward the end of the events (see Figure 3–6), the frequency of longer high-pressure blocking events was also examined. However, no increase could be observed in any of the cases. More interestingly a small decrease can be observed from the  $\tau$ -values and the Sen's slope values. However one must note that the p-values are much larger here than Figure 3–6, indicating a more random system.

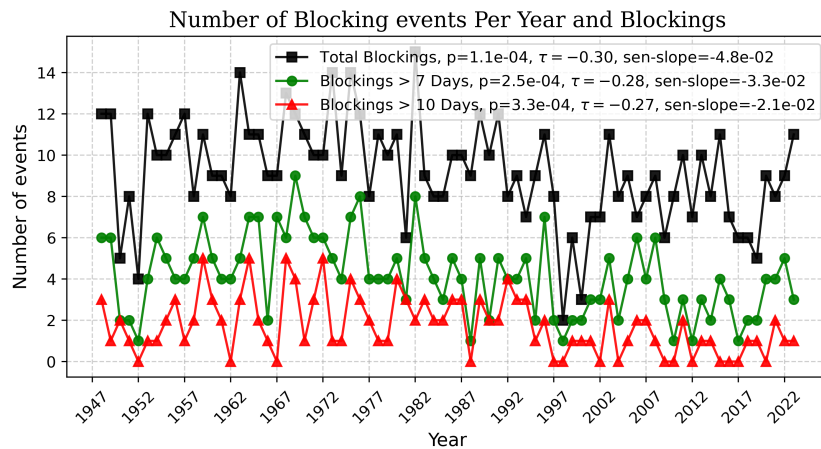


Figure 7: This plots shows the change in frequency of high-pressure blocking events. The plots also indicates the change in events longer than seven and ten days.

In Figure 8, the number of days with high-pressure blocking events per year can be seen. Here, the total, seasonal, and pressure strength dependence can be observed. The reason for not including the directional dependence is that no wind data was available for this period. Even here a slight decrease can be seen in most plots, especially the total blocking days per year (h).

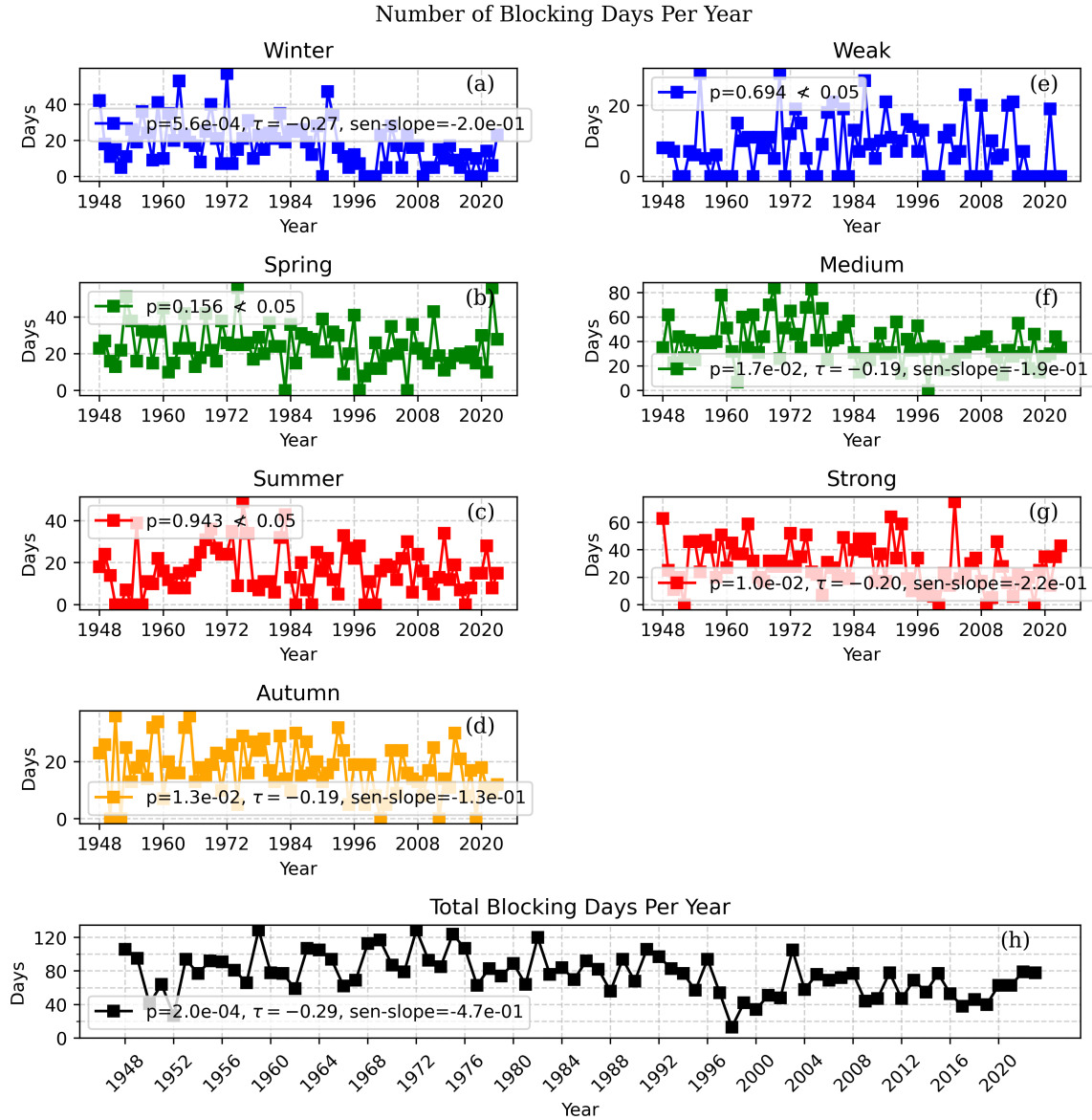


Figure 8: Plots showing the change in frequency of days under high-pressure blocking events. The number of days under a high-pressure blocking event each year, during each season, and for different pressure strengths can also be seen.

When observing slight decline of the frequency of the high-pressure blocking events in Figure 7 and Figure 8 one must note that the low  $|\tau|$ -values indicate that the trend is not monotonic. Furthermore, the large p-values indicate that the trend is more random in comparison to the mean aerosol concentration plots observed in Figures 3–6. This indicates that this trend is more likely caused to randomness, and should not be seen as a result. However, one can observe that no type of high-pressure blocking events has become more common during the last 74 years. This is an interesting result since the opposite has been found in western Europe [3].

## 4 Discussion

### 4.1 Why an Increase Occurs After 8-13 Days for Stronger High-Pressure Systems

The result above showed that for all high-pressure blocking events, except for events with winds from the northeast, an aerosol increase was seen after eight to thirteen days compared to the initial aerosol values. This outcome provides an important result, which is that the aerosol concentration accumulates during high-pressure blocking events. An interesting observation is that this occurs after this specific time.

### 4.2 Particle Advection Versus Local Emissions

One important concept to discuss is whether the accumulation of aerosol is due to local emissions or particle advection from other locations. To address this question, several observations can be made: Firstly, local emissions in urban Malmö should be much higher than those in rural Vavihill. Secondly, if the increase is due to particle advection, the increase should depend strongly on the wind direction.

From all the plots regarding PM<sub>2.5</sub>, one can observe that the increase in Malmö is generally stronger than in Vavihill. This suggests, as predicted, that some of the increase in aerosol is due to local emissions. One could argue that this increase might be due to other factors, such as the fact that Malmö is coastal, whereas Vavihill is not, or that Malmö is located near regions with higher emissions, such as central Europe. However, this is unlikely to be the case. Firstly, the fact that Malmö is coastal would not suggest a higher aerosol increase than in Vavihill. The coastal factor may influence the overall air quality in the location, but since we are observing local changes, this factor should be accounted for. The argument that Malmö is more closely located to central Europe, especially in the southeastern direction may play a role in the stronger increase in Malmö than Vavihill. This is due to the fact that stronger high-pressure blocking events indicate more stagnant air which would imply that locations closer to the locations of high emission would be impacted more strongly than locations further away. However, the length scale to central Europe compared to the length scale between Vavihill and Malmö makes this factor irrelevant. Furthermore, other large urban areas such as Copenhagen are not closer to Malmö than Vavihill.

If we examine the wind dependence, we observe another interesting result. For wind direction from the northeast, there is no noticeable increase in aerosols, whereas we see a stronger increase when the wind comes from the west, and an even stronger increase from the southeastern direction. This suggests that some of the particle increase is due to particle advection. More importantly, we observe a notable difference between the southeastern and the northeastern directions. One could argue that this directional increase has more to do with the different types of high-pressure blocking events. However, the main difference between different types of high-pressure blocking

events is where they are centred, which mainly correspond to different wind directions.

Another argument which indicates that there is a directional dependence is comparing the data from the non-specified wind direction with the other wind directions. The non-specified wind direction showed a monotone increase for both locations; however, this increase is not as strong as the increase observed for the southeastern direction. Furthermore, the northeast direction showed a smaller increase than the non-specified direction. The non-specified direction could be the increase corresponding to the local emission, whereas the directional plots show how the local particle concentration is affected by the particles arriving with the wind. This would suggest that the wind from the northeast contains cleaner air, whereas the wind from the southeast is exhibiting a higher aerosol concentration.

### 4.3 Differences Between the Urban and Rural Locations

In the plots above one could observe that the aerosol accumulation was stronger in the case for the urban location in comparison to the rural. Several reasons could explain this behaviour. Firstly, emissions in the urban location should be higher than in the case of the rural location. This is supported by the seasonal dependence where similar behaviour of the aerosol concentrations is seen for both locations except during the winter, where a larger increase is seen in the urban location. Since aerosols emissions increase due to domestic heating during the winter would one expect a stronger increase in the urban location during the winter.

Another reason might be the difference in the inversion layer for the different locations. Although the natural description of the two locations are similar, the skyline due to buildings is not. The urban location has many buildings which hold moisture badly, whereas the rural is characterised by nearby trees and hills which are better at holding moisture. This makes the ground more dependent on the ground radiation, which results in a clearer ground inversion layer in the urban location. One would thus obtain more vertical air mixture in the rural location, which would contribute to the lower levels of aerosols in this location.

However, since the aerosol levels mainly differ during the winter, one could note that the main difference between the rural and the urban location is the local emissions. One could argue that the ground inversion during the winter is amplified due to longer nights, which would amplify the inversion layer and prevent further air mixing. However, since the inversion is mainly affected by the subsidence inversion, which is similar for the two locations, one would not see a large difference between the two locations. So, although this may contribute to the higher levels of aerosols during the winter, it would not explain the difference between the urban and rural locations. One can thus conclude although there is a slightly stronger ground inversion in the urban location, the larger emissions of the urban location mainly a consequence of the higher emissions.

## 5 Conclusion

This thesis has demonstrated that the presence of high-pressure blocking events in southern Sweden significantly increased the aerosol concentration in both rural and urban locations. The PM<sub>2.5</sub> mean increase in Malmö went from 10 µg m<sup>-3</sup> to a maximum of 21 µg m<sup>-3</sup> during the high-pressure blocking period, and an increase from 7 µg m<sup>-3</sup> to a maximum of 18 µg m<sup>-3</sup> could be observed in Vavihill. Increased levels of PM<sub>2.5</sub> were seen in both locations after eight to thirteen days of uninterrupted high-pressure blocking, indicating accumulation of aerosols during the events. This accumulation was mainly attributed to the presence of a subsidence inversion layer, which prohibited vertical air mixing. A stronger increase was found in the urban area of Malmö than the rural area of Vavihill, which was mainly attributed to local emissions. The wind directional dependence on PM<sub>2.5</sub> concentrations indicated that the long-range advection of aerosols was a significant contributor to aerosol concentration in the region, where winds from central and eastern Europe significantly increased the aerosol levels, whereas winds from the northeast did not affect the concentrations. The seasonal dependence indicated an increase during the winter, which supports the idea of local emissions affecting the aerosol concentration. A stronger increase was also observed with stronger high-pressure blocking events, where the highest levels of PM<sub>2.5</sub> could be observed. Observing the lengths and number of high-pressure blocking events showed that there has not been an increase of any sort during the last 74 years, which differs from other European studies on nearby regions.

## 6 Outlook

Future work on this subject should use a more advanced classification of different types of high-pressure blocking events by using data from multiple meteorological stations. This would create a clearer view of the actual movement of the anticyclone, which could be used to simulate the advection of aerosols. Comparing this simulation with the values from this thesis would give more insight into the actual advection of the aerosols. To study local emissions, one could monitor the local emission and compare this to the aerosol concentrations during high-pressure blocking events to see the effect that these play. To analyse the role of the inversion layer during the event, one could monitor vertical atmospheric data to see the effect of the subsidence inversion on the aerosol concentrations.

To summarize, the analysis of aerosol concentrations during meteorological events is important for monitoring the health risks associated with different meteorological phenomena. This thesis has shown that not only domestic emissions play a role in air quality, but that advection from nearby countries also plays a crucial role. This shows the magnitude of international work to prohibit the large-scale emissions of aerosols. As the climate changes, so does the weather, and understanding how this affects us is of the utmost importance.

## References

- [1] NASA. Haze over Europe. <https://earthobservatory.nasa.gov/images/11219/haze-over-europe>, March 2003.
- [2] John F. B. Mitchell, Jason Lowe, Richard A. Wood, and Michael Vellinga. Extreme events due to human-induced climate change. *Philosophical Transactions of the Royal Society A: Mathematical, Physical and Engineering Sciences*, 364(1845):2117–2133, 2006.
- [3] Anthony R. Lupo. Atmospheric blocking events: A review. <https://doi.org/10.1111/nyas.14557>, December 2020.
- [4] Wenyue Cai, Xiangde Xu, Xinghong Cheng, Fengying Wei, Xinfia Qiu, and Wenhui Zhu. Impact of “blocking” structure in the troposphere on the wintertime persistent heavy air pollution in northern China. *Science of The Total Environment*, 741:140325, 2020.
- [5] Vlado Spiridonov and Ćurić Mladjen. Cyclones and Anticyclones | SpringerLink. [https://link.springer.com/chapter/10.1007/978-3-030-52655-9\\_17](https://link.springer.com/chapter/10.1007/978-3-030-52655-9_17), November 2020.
- [6] E. Gramsch, D. Cáceres, P. Oyola, F. Reyes, Y. Vásquez, M. A. Rubio, and G. Sánchez. Influence of surface and subsidence thermal inversion on PM<sub>2.5</sub> and black carbon concentration. *Atmospheric Environment*, 98:290–298, December 2014.
- [7] Greg O’Hare, Rob Wilby, and John Sweeney and Rob Wilby. *Weather, Climate and Climate Change*. Pearson Eductaion Limited, England, 2005.
- [8] Magdalena Porębska and Małgorzata Zdunek. Analysis of extreme temperature events in Central Europe related to high pressure blocking situations in 2001–2011. *Meteorologische Zeitschrift*, 22(5):533–540, 2013.
- [9] Judit Bartholy, Rita Pongracz, and Margit Pattantyús-Ábrahám. European Cyclone Track Analysis Based on ECMWF ERA-40 Data Sets. *International Journal of Climatology*, 26(11):1517–1527, 2006.
- [10] Noelia Otero, Oscar E. Jurado, Tim Butler, and Henning W. Rust. The impact of atmospheric blocking on the compounding effect of ozone pollution and temperature: A copula-based approach. *Atmospheric Chemistry and Physics*, 22(3):1905–1919, 2022.
- [11] European Environment Agency. Europe’s air quality status 2024. <https://www.eea.europa.eu/publications/europees-air-quality-status-2024>, 2024.
- [12] Shubham Sharma, Mina Chandra, and Sri Harsha Kota. Health Effects Associated with PM<sub>2.5</sub>: A Systematic Review. *Current Pollution Reports*, 6(4):345–367, 2020.
- [13] Ulla Arthur Hvidtfeldt, Mette Sørensen, Camilla Geels, Matthias Ketzel, Jibran Khan, Anne Tjønneland, Kim Overvad, Jørgen Brandt, and Ole Raaschou-Nielsen. Long-term residential exposure to PM<sub>2.5</sub>, PM<sub>10</sub>, black carbon, NO<sub>2</sub>, and ozone and mortality in a Danish cohort. *Environment International*, 123:265–272, February 2019.

- [14] A. Analitis, P. Michelozzi, D. D’Ippoliti, F. De’Donato, B. Menne, F. Matthies, R. W. Atkinson, C. Iñiguez, X. Basagaña, A. Schneider, A. Lefranc, A. Paldy, L. Bisanti, and K. Katsouyanni. Effects of heat waves on mortality: Effect modification and confounding by air pollutants. *Epidemiology*, 25(1):15–22, 2014.
- [15] Sigler, Marian. Blank map of Europe (with disputed regions). [https://commons.wikimedia.org/wiki/File:Blank\\_map\\_of\\_Europe\\_\(with\\_disputed\\_regions\).svg](https://commons.wikimedia.org/wiki/File:Blank_map_of_Europe_(with_disputed_regions).svg), February 2007.
- [16] Thermo Fisher Scientific Inc. TEOM® Series 1400a Ambient Particulate (PM-10) Monitor Operating Manual, 2007.
- [17] PALAS GmbH. Operating Manual: Fidas® Fine Dust Monitor System.
- [18] Thermo Scientific. 8500 FDMS Filter Dynamics Measurement System, 2010.
- [19] VAISALA. PTB 200 DIGITAL BAROMETERS USER’S GUIDE, February 1993.
- [20] VAISALA. PTB220 Series Digital Barometers USER’S GUIDE, August 2001.
- [21] VAISALA. Wind Set WA15 and WA25. <https://www.vaisala.com/en/products/weather-environmental-sensors/wind-set-wa15>, January 2021.
- [22] GEONOR, Inc. T-200B Series All Weather Gauge. <https://www.geonor.com/t-200b-all-weather-precipitation—rain-gauge>, 2019.
- [23] Hussain, Md. and Mahmud, Ishtiaq. pyMannKendall: A python package for non parametric Mann Kendall family of trend tests. *Journal of Open Source Software*, 4(3):1556, July 2019.

